

Cite this: *Phys. Chem. Chem. Phys.*, 2011, **13**, 2850–2856

www.rsc.org/pccp

PAPER

Charge carrier mobility in poly[methyl(phenyl)silylene] studied by time-resolved terahertz spectroscopy and molecular modelling[†]

Hynek Němec,^a Irena Kratochvílová,^{*a} Petr Kužel,^a Jakub Šebera,^{b,c}
Anna Kochalska,^b Juraj Nožár^b and Stanislav Nešpůrek^b

Received 2nd June 2010, Accepted 22nd October 2010

DOI: 10.1039/c0cp00774a

Time-resolved terahertz spectroscopy and combination of quantum chemistry modeling and molecular dynamics simulations were used for the determination of charge carrier mobility in poly[methyl(phenyl)silylene]. Using time-resolved THz spectroscopy we established the on-chain charge carrier drift mobility in PMPSi as $0.02 \text{ cm}^2 \text{ V}^{-1} \text{ s}^{-1}$. This value is low due to the formation of polarons: the hole is self-trapped in a potential formed by local chain distortion and the transient THz conductivity spectra show signatures of its oscillations within this potential well. This view is supported by the agreement between experimental and calculated values of the on-chain charge carrier mobility.

1. Introduction

Molecular materials represent the ultimate step in device miniaturisation with the advantage of an almost unlimited possibility to tailor their physical properties. The charge transport in molecular electronic materials is a very complex process which can be affected by many physical and chemical parameters; the knowledge of its nature is crucial for the development and optimization of molecular-based devices. Each step forward in understanding and controlling the charge transport is extremely important for the practical applications of molecular systems in electronics. Molecular wires can serve as connectors between electronic elements and conjugated polymer chains can be used for this purpose.^{1,2} On-chain charge carrier mobility then appears as the fundamental parameter controlling the performance of the wires.³

In this paper we focus on polysilanes as polymers with a σ -conjugation in the backbone. They are of considerable research interest because of their electronic, photoelectric and nonlinear optical properties.^{4,5} Time-resolved terahertz spectroscopy and density functional theory calculations were employed for the investigation of on-chain charge mobility in poly[methyl(phenyl)silylene] (PMPSi). Given its relatively high frequency the THz spectroscopy probes the charge transport and localization on a nanoscopic length scale^{6,7} and, since

recently, it has provided pertinent answers on ultrafast charge carrier dynamics in a large variety of systems.^{6,8,9} It is also appealing that THz spectroscopy is sensitive to the intra-chain transport whereas most of the classical electrical methods probe the conductivity limited by inter-chain transport.¹⁰ The experimental sensitivity to structural and static conformational defects on the backbone can be increased if lower probing frequencies are used.¹¹ A comparison of THz mobilities with those obtained recently by a time-resolved microwave conductivity technique allows us to elucidate the role of such defects.^{4,12}

In order to further support the proposed mechanisms of the charge carrier transport along the PMPSi chain, computer molecular modelling was also performed. To the best of our knowledge, calculations of PMPSi on-chain charge carrier mobility have not been published yet.

2. Experimental

2.1 Material and sample preparation

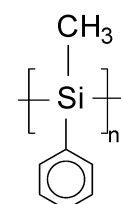
Poly[methyl(phenyl)silylene] (PMPSi, see Scheme 1) was synthesised by a Wurtz coupling of distilled dichloro-(methyl)phenylsilane by sodium metal in dried toluene containing 15% n-heptane in an inert atmosphere in the dark. The insoluble part of the polymer (mostly crosslinked PMPSi)

^a Institute of Physics AS CR, Na Slovance 2, 182 21 Prague 8, Czech Republic. E-mail: krat@fzu.cz; Fax: (+420) 286 890 527; Tel: (+420) 266 052 126

^b Institute of Macromolecular Chemistry AS CR, Heyrovského nám. 2, 162 06 Prague 6, Czech Republic

^c J. Heyrovský Institute of Physical Chemistry AS CR, Dolejškova 3, 182 23 Prague 8, Czech Republic

† Electronic supplementary information (ESI) available: Overview of the calculations of the electron transfer Integral (Tables S1 and S2). See DOI: 10.1039/c0cp00774a



Scheme 1 Chemical structure of poly[methyl(phenyl)silylene].

was removed by centrifugation, after which the polymer was precipitated with excess methanol, filtered off and dried in vacuum. The low-molecular-weight cyclic oligomers were removed by boiling the precipitate in diethylether. PMPSi was filtered off and dried in vacuum at 40 °C for 24 h. The material was characterised by a Perkin Elmer Lambda 20 spectrophotometer and GP chromatography. The characteristic absorption maximum of the (σ - σ^*) transitions was located at 340 nm, that of the (σ - π^*) transitions at 277 nm (measured in tetrahydrofuran solution). The molar mass was determined as $M_w = 20\,074 \text{ g mol}^{-1}$, $M_n = 8355 \text{ g mol}^{-1}$.

Two kinds of PMPSi samples were investigated: thin solid films deposited on fused silica substrates and a 1.8 mM suspension in tetrachloromethane. The thin films were prepared from a toluene solution by a spin-coating method.

2.2 Time-resolved THz spectroscopy

The THz conductivity spectra of the samples were measured using optical pump–THz probe spectroscopy.^{6,13} We employed the setup described in detail in ref. 14 which was based on a Ti:sapphire femtosecond laser amplifier providing 60 fs pulses with a mean wavelength of 810 nm and the energy of 1 mJ per pulse. The pulse train was split into three branches (see Fig. 1). The beam in the first one was frequency tripled and the resulting wavelength of 270 nm was used for the photoexcitation of the sample (pump). The second branch was used for the generation of broadband picosecond THz pulses *via* optical rectification in a 1 mm thick [011] ZnTe crystal.¹⁵ These pulses (propagating in the free space) were used for the probing of the transient optical absorption of the samples in the range of 0.2–2.0 THz (wavelength 0.15–1.5 mm) in the pump–probe experiment. The third (sampling) branch served for the phase-sensitive detection of the transmitted THz field in another [011] ZnTe crystal using the gated electro-optic detection scheme.¹⁵

We employed the excitation photon flux of $\Phi = 4 \times 10^{14} \text{ photons cm}^{-2}$ per pulse.¹⁶ On the investigated time scale (picoseconds), the excitations do not have enough time to meet each other; consequently, any interaction between them can be neglected. The thin film samples were placed in a low-vacuum chamber for the measurements and the employed

excitation fluence did not lead to any visible damage of the films. The PMPSi suspension was investigated in a 1 mm thick quartz flow cell. This eliminated bleaching of the suspension upon illumination by the laser beam, which otherwise occurred in a static cell. However, even in the flow cell, we observed the formation of a sediment on the cell walls after a few hours of laser irradiation. All measurements were performed at room temperature (293 K).

Time-resolved THz spectroscopy requires two measurement steps: (i) measurement of the temporal profile (wave-form) of the electric field $E_0(t)$ of the picosecond THz pulse transmitted through an unexcited sample (reference wave-form) and (ii) that of the transient field $\Delta E(t, \tau_p)$, representing the change in the wave-form $E_0(t)$ induced by the photo-excitation at the pump–probe delay τ_p . The Fourier transformation of the wave-forms provides complex spectra of these pulses $\Delta E(f, \tau_p)$ and $E_0(f)$ and their ratio, $\Delta E(f, \tau_p)/E_0(f)$, represents the transient transmittance of the sample. In the quasi-steady-state approximation (which applies for dynamics slower than $\sim 1 \text{ ps}$) and for a weak photo-induced signal ($\Delta E \ll E_0$) the transient transmittance is simply proportional to the transient optical conductivity $\Delta\sigma$ in the THz range:^{14,17}

$$\frac{\Delta\sigma(f, \tau_p)}{n_{\text{exc}}e} = -(1 + N_s) \cdot \frac{\Delta E(f, \tau_p)}{E_0(f)} \cdot \frac{ce_0}{e\Phi} \quad (1)$$

where c is the speed of light in vacuum, ε_0 is the vacuum permittivity, N_s is the THz refractive index of the substrate, e is the elementary charge, and n_{exc} is the excitation density (number of absorbed photons per pump laser pulse and per unit volume). Expression (1) is a thin-film limit of a general relation between $\Delta\sigma$ and $\Delta E/E_0$ derived in ref. 17; this limit assumes that the film thickness is much smaller than the THz wavelength of the probe pulse and that the pump pulse is entirely absorbed by the sample. The left-hand side of eqn (1), $\Delta\sigma/(n_{\text{exc}}e)$, is the key quantity provided by time-resolved THz spectroscopy: it is the product of the quantum yield ξ of the formation of mobile charge carriers and of their mobility μ .⁸

We emphasize that time-resolved THz spectroscopy is a phase sensitive method which makes it possible to measure

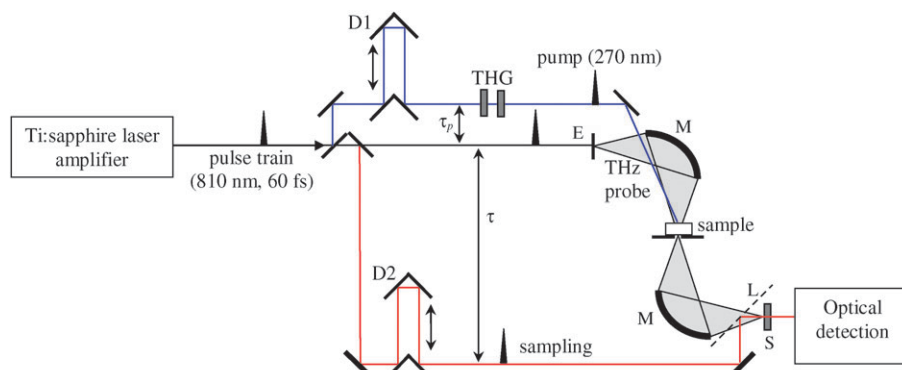


Fig. 1 Scheme of the experimental setup for time-resolved THz spectroscopy. D1—motorized stage for controlling the pump-probe delay (τ_p), THG—two β -barium borate (BBO) crystals for third harmonic generation, E—emitter (ZnTe crystal for conversion of the near infrared pulses into pulses of THz radiation by optical rectification),¹⁵ M—ellipsoidal mirrors, D2—motorized stage for scanning the THz pulse profile, L—pellicle beam-splitter, S—sensor (ZnTe crystal for electro-optic detection of THz pulses).¹⁵

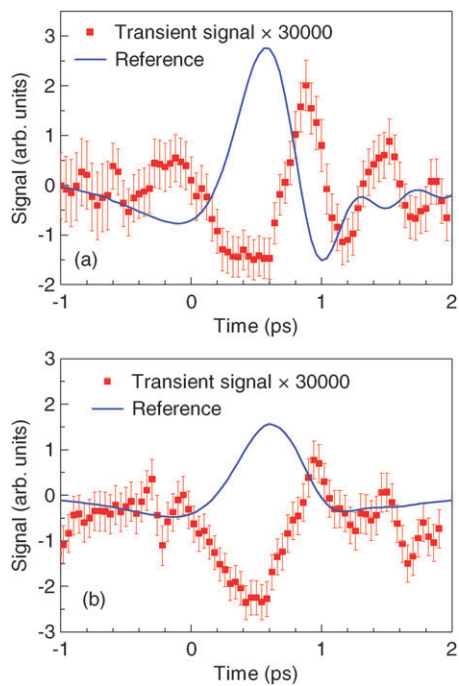


Fig. 2 Reference wave-form transmitted through the sample without photo-excitation (solid line) and its change induced by the photo-excitation (symbols) for (a) PMPSi solid film and (b) PMPSi suspension in CCl₄. The pump–probe delay was 10 ps in both cases. The error bars correspond to the standard deviation of the average values.

the *complex* transient transmittance and to evaluate the *complex* transient conductivity $\Delta\sigma$:

$$\Delta\sigma = \Delta\sigma_1 + i\Delta\sigma_2 \quad (2)$$

or, equivalently, the *complex* electric permittivity $\Delta\epsilon = -\Delta\sigma/(2\pi if_0)$ which both express the interaction of THz probing radiation with localized and delocalized carriers. The real conductivity spectrum $\Delta\sigma_1$ represents losses (usually of ohmic character) and its extrapolation to zero frequency characterizes the on-chain drift mobility of charges in our sample. The imaginary part of the conductivity (or real part of the permittivity) reflects the polarizability and inductance of localized and delocalized charges. In this sense, the retrieved information is richer in comparison with the methods using infrared or visible probing light: these techniques typically detect the change in the transmitted optical power which merely provides the change in the absorption coefficient. The (optical) conductivity measured by THz spectroscopy describes the charge motion over <50 nm and should not be confused with the dc conductivity characterizing the charge transport over macroscopic distances (which includes in addition, *e.g.*, the charge hoping between polymer chains).

The measured time-domain THz wave-forms are shown in Fig. 2. The photo-induced signal was extremely weak, about 30 000 times weaker than the reference signal. To achieve this sensitivity of the measurements a very long data acquisition process was required. A sufficient signal-to-noise ratio was obtained after 14 and 8 h of data averaging for the wave-forms

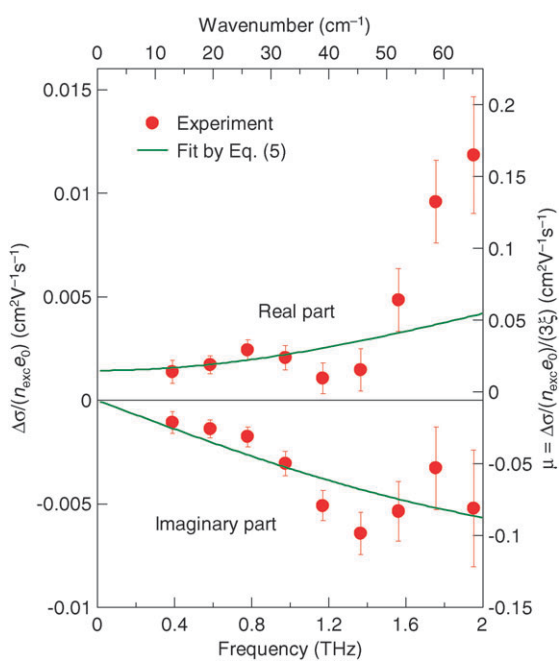


Fig. 3 Normalized transient conductivity spectra of the PMPSi solid film for the pump–probe delay 10 ps.

shown in Fig. 2a and b, respectively. For this reason, conductivity was measured for a single pump–probe delay ($\tau_p = 10$ ps). We observed that the transient wave-forms did not reproduce exactly the shape of the reference wave-forms: they were somewhat distorted. This is related to the dispersion in the conductivity spectra. Note that, for the PMPSi suspension, the high-frequency spectral components were significantly suppressed because of the absorption of THz radiation in CCl₄.¹⁸ This prevented us from a reliable retrieval of the transient conductivity for the suspension. The suppression of high-frequency components is also responsible for broadening of the reference THz wave-form transmitted through the suspension (Fig. 2b) as compared to that presented in Fig. 2a for the solid film. The transient conductivity spectrum of the film calculated using eqn (1) is shown in Fig. 3.

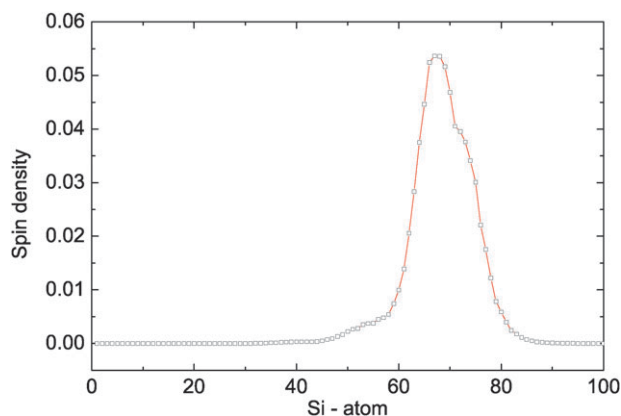


Fig. 4 Spin distribution on the Si-chain 200 fs after photoexcitation as obtained by molecular dynamics simulations.

3. Computer modelling

3.1 Molecular dynamics

The aim of molecular dynamics (MD) modelling was to simulate the evolution of PMPSi chain deformation induced by an insertion of a positive charge. Quenched molecular dynamics simulations were performed using Materials Studio,¹⁹ Version 4.3.0.0, with a polymer consistent force field.²⁰ The spin distribution on the Si-backbone in cation-radical state was calculated by the Gaussian 09 package using the Extended Hückel method.

At time zero, the structure of PMPSi was assumed to be a regular all-*trans* form. After thermal activation and insertion of a positive charge (hole), the Si backbone started to deform gradually. It was found that a localised distortion (polaron) is formed within tens of femtoseconds extending about 20MPSi monomer units. This is illustrated by the spin-density plot in Fig. 4.

The obtained localization length is in good agreement with the value obtained by Tachikawa,²¹ who performed MD modelling of a similar polymer (dimethylsilane) using the quantum semi-empirical method AM1. Irie *et al.* measured the electron absorption spectra of radical ions of oligo- and poly(methyl-propylsilane)s in rigid matrices at 77 K.²² They found that the spectra are saturated at 16 units.

3.2 Density functional theory

The electronic structures and equilibrium geometries of neutral oligomers of different lengths (up to 20 MPSi monomer units) were calculated with the DFT method using the Gaussian 09 program package.²³ The DFT calculations employed hybrid functionals: B3LYP²⁴ and CAM-B3LYP.²⁵ The Coulomb-attenuating method (CAM-B3LYP) improves the B3LYP functional and combines the hybrid qualities of B3LYP with the long-range correction presented by Tawada *et al.*²⁶ The CAM-B3LYP functional comprises 0.19 Hartree–Fock (HF) plus 0.81 Becke 1988 (B88) exchange interaction at short range, and 0.65 HF plus 0.35 B88 at long range. For the description of the parameters of Si, H and C atoms, the polarised double basis set 6-31G* was used.²⁷ For the electron-transfer calculations, the H atoms were described by 3-21G* because the calculations of orbital transformations are then less time consuming.²⁸

The essential parameter controlling the charge mobility is the charge transfer integral. Here, we evaluate the transfer integral for the hole transfer from the deformed to a close undeformed part of the chain. We first calculated the conformation of the positive polaron on PMPSi deformed chains of different lengths using the unrestricted Kohn–Sham method. The orbitals localised over half of the chain were calculated using the Corresponding Orbital Transformation method.²⁸ It is crucial to ensure that the electron transfer (ET) reactant and product wave functions reflect the localised states.^{29–33} The transfer integral t^+ for the hole transfer was calculated according to the formula³⁴

$$t^+ = \frac{H_{RP} - S_{RP}(H_{RR} + H_{PP})/2}{1 - S_{RP}^2}, \quad (3)$$

where H_{RP} is the interaction energy between reactant and product states, S_{RP} is the overlap between the reactant and product states and H_{RR} is electronic energy of the reactant state and H_{PP} is electronic energy of the product state. All these terms were obtained *via* the direct coupling of localised orbitals. The calculation of t^+ was implemented in the NWChem quantum chemistry package³⁵ using the Marcus two-state transfer model^{36–38} (for details see the ESI).† Localised molecular orbitals were calculated by the unrestricted Hartree–Fock method as DFT calculations have not been implemented in NWChem program.

On the molecular level, three factors, the electronic coupling (transfer integral t^+) between the individual parts of the molecule, the reorganisation energy λ^+ during charge transport and the effective length of hole transfer L , are usually considered to be important for charge transport in organic materials.^{39,40}

The reorganization energy λ^+ consists of the sum of λ_1^+ and λ_2^+ , $\lambda^+ = \lambda_1^+ + \lambda_2^+$, where the deformation energy of the system λ_1^+ was calculated as the difference between the vertical and cationic state: $\lambda_1^+ = E_+(Q_N) - E_+(Q_+)$ and $\lambda_2^+ = E_N(Q_+) - E_+(Q_N)$. Here, $E_+(Q_N)$ is the total electronic energy of the cationic state in the neutral geometry, $E_+(Q_+)$ is the total energy of the cationic state geometry, $E_N(Q_+)$ is the total energy of the neutral state in the cationic state geometry and $E_N(Q_N)$ is the total energy of the neutral state in the neutral geometry see Fig. S4 in the ESI.†

At room temperature, the charge carrier transport can be described within the Marcus theory.^{41–45} Subsequently, the rate of a self-exchange process was provided by the expression

$$k_{et} = \frac{2\pi}{\hbar} \frac{1}{\sqrt{4\pi\lambda^+ kT}} (t^+)^2 \exp\left(-\frac{\lambda^+}{4kT}\right), \quad (4)$$

where \hbar is the reduced Planck constant, k is the Boltzmann constant, T is the temperature and λ^+ is the reorganisation energy. The diffusion coefficient D of charge carriers can be expressed using the Einstein-Smoluchowski equation

$$D = L^2 k_{et}. \quad (5)$$

This makes it possible to evaluate the on-chain drift mobility of the charge carriers^{46–48} using the Einstein relation $\mu = eD/kT$. It should be noted that the calculated charge mobility mentioned here represents the zero electric field approximation value. More details of electron transfer calculations and reorganization energy calculations are summarized in the ESI.†

4. Discussion

UV photo-excitation leads to a rapid formation of an electron-hole pair on a polymer chain.⁴⁹ The most probable electron-hole separation distance in this state is 2.9 nm (= 12 a_{Si-Si}).⁵⁰ The electron-hole pairs either recombine geminately or dissociate *via* an Onsager mechanism and give rise to free charge carriers.^{51,52} Within 10 ps after the photoexcitation, the pairs do not have a chance to recombine or dissociate which means that we are dealing with a system in an on-chain charge transfer state. Electrons are localised on phenyl groups and do

not contribute to the THz conductivity. Their recombination with holes occurs on a microsecond time scale¹⁶ and, consequently, this process can be neglected in our considerations.

From Fig. 3 we observe that the real part of the transient conductivity is very low at low frequencies, but it does not vanish completely.⁵³ It slightly increases with increasing the frequency, whereas the imaginary part is negative. This response is characteristic of localised charges, and the spectrum can be phenomenologically understood in terms of the response of a damped harmonic oscillator.⁶ Thus, we describe the transient conductivity spectrum as the sum of two terms. The first one contains a low-frequency mobility μ_1 , representing the on-chain drift of charge carriers, and the second one contains the parameters characterising the oscillator:

$$\Delta\sigma(f) = \frac{1}{3}ne\mu_1 + \frac{1}{3}\frac{ne^2}{2\pi m} \left(-\frac{if}{f_0^2 - f^2 - i\gamma f/(2\pi)} \right), \quad (6)$$

where n is the density of available electron-hole pairs, m is the charge mass, f_0 is the resonant frequency of the oscillator and γ is the oscillator damping. The factor of 1/3 accounts for the fact that the polymer chains are randomly oriented in the samples in three dimensions. The electron-hole pair density n in eqn (6) equals ξn_{exc} , where the primary quantum yield ξ expresses the quantum yield of pairs shortly after the photoexcitation. For PMPSi, the primary quantum yield of $\xi = 0.2$ was determined⁵⁰ by the technique of emission-limited photoinduced discharge^{54,55} (the saturated yield value measured in high electric fields is taken into account since it represents the primary yield of the non-separated electron-hole pairs). These considerations allow us to estimate the hole mobility spectra from our experiment (the right-hand axis in Fig. 3). Extrapolation of $\text{Re } \Delta\sigma$ to zero frequency provides the estimation of the on-chain hole mobility $\mu_1 \sim 0.02 \text{ cm}^2 \text{ V}^{-1} \text{ s}^{-1}$; from the fit of the slope of $\text{Im } \Delta\sigma$ vs. frequency, the parameter $f_0 \sim 80 \text{ THz}$ was obtained (the solid line in Fig. 3). Our mobility value is in good agreement with that measured by the time-resolved microwave conductivity technique.^{56–58} In ref. 57 and 58, the mobility was calculated from recombination kinetics and a value of $0.02 \text{ cm}^2 \text{ V}^{-1} \text{ s}^{-1}$ was reported. Thus, we can state that the on-chain charge carrier mobilities in the microwave region and in the low-frequency part of the THz range are practically the same. This shows that energy barriers, such as conjugation defects, have no influence on the hole transport for frequencies above a few GHz,^{11,59} *i.e.*, the measured microwave and THz mobilities represent the intrinsic on-chain drift mobilities of the holes (unaffected by the static defects).

The very low value of the mobility ($\ll 1 \text{ cm}^2 \text{ V}^{-1} \text{ s}^{-1}$) rules out the band transport model.⁶⁰ From our measurements in the THz spectral range, we infer that the ‘band conductivity’ is not a dominating transport mechanism even locally. In ref. 59 it was shown that even infinite potential barriers located between each quadruplet of polymer repeat units do not suppress the mobility below a value of $0.45 \text{ cm}^2 \text{ V}^{-1} \text{ s}^{-1}$. The much lower value of the mobility observed in PMPSi may be related to the formation of polarons in agreement with the molecular dynamics simulations. The mobile hole photogenerated on the silicon chain induces local chain

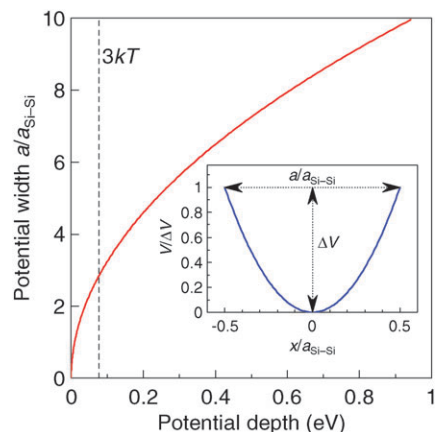


Fig. 5 Relation between the possible depth and width of the harmonic potential with resonant frequency $f_0 = 80 \text{ THz}$. Inset: Potential profile. The distance between the MPSi units $a_{\text{Si-Si}} = 2.35 \text{ \AA}$.

distortion where it is self-trapped. The on-chain transport of holes is then necessarily related to the dynamic change of the polaron potential accompanying the hole motion which strongly reduces drift mobility. On the other hand, we can also regard the lattice distortion as a potential well, in which the hole oscillates—this is supported by the observed oscillator response. To get an idea of the polaron properties, we assume that the hole oscillates inside a harmonic potential well with a depth ΔV and a width a , *i.e.*, $V(x) = 4\Delta V x^2/a^2$ (see Fig. 5). The resonant frequency f_0 then reads

$$f_0 = \sqrt{\frac{2\Delta V}{m\pi^2 a^2}}. \quad (7)$$

Since we have determined the resonant frequency from the fit of the transient conductivity spectra, this expression constitutes a link between the polaron size (width a) and a binding energy (depth ΔV), see Fig. 5. The polaron binding energy must be much larger than 3 kT , otherwise the charge carrier would escape the well, which would lead to the disappearance of the oscillator response and appearance of

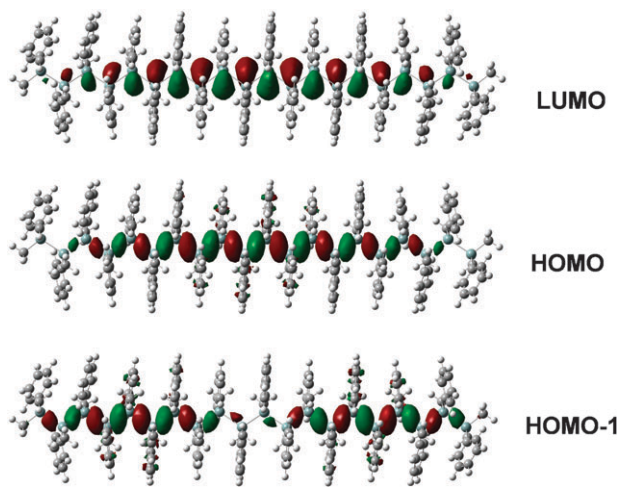


Fig. 6 Schematic representation of the two highest lying occupied orbitals HOMO and HOMO-1 and the lowest lying unoccupied orbital LUMO of 20-mer of methyl(phenyl)silylene (20MPSi).

Drude-like response of free charge carriers. From Fig. 5, we can thus determine that the polaron size a is at least $3a_{\text{Si-Si}}$ on the time scale of 10 ps.

The photoinduced THz signals in a PMPSi film and solution are comparable (Fig. 2a and b, respectively). There is no essential discrepancy in the transport parameters obtained for the solid films and solutions. Thus, one can assume little influence of the chain morphology and local environment on the charge transport in PMPSi molecules on the picosecond time scale. Unlike in, *e.g.*, poly[methoxy-5-(2'ethyl-hexyloxy)-1,4-phenylene vinylene] semiconducting polymer, the interchain charge carrier transport effects are not crucial in an ultrafast time scale.¹⁰

We supposed that HOMO and HOMO-1 can create transport orbitals. The HOMO, HOMO-1 and LUMO orbitals are localised on Si atoms, see Fig. 6. The results of the calculations obtained from molecular dynamics simulations showed that the hole is localised on about 20 monomer units (Fig. 4). This localisation length is in a good agreement with ref. 21. A deformation energy λ_1^+ of 0.25 eV and reorganisation energy λ^+ of 0.55 eV were calculated for the oligomer containing 20 units. B3LYP calculation of the deformation energy λ_1^+ gives for large systems (in our case 20 units) a rather underestimated value of 0.11 eV. Experimental deformation energy is equal to 0.22 eV.^{61,62} For 40 units the transfer integral value was found as 3.4 meV (for details see the ESI†).⁶³ For the hole transfer distance $L = 20a_{\text{Si-Si}}$, we receive from eqn (4) and eqn (5) the on-chain hole mobility of $7 \times 10^{-3} \text{ cm}^2 \text{ V}^{-1} \text{ s}^{-1}$. This result is in quite a good agreement with the mobilities obtained by microwave techniques as well as with value measured by transient THz spectroscopy. Thus, from our experimental and theoretical results agreement we can conclude that charge (delocalised hole) transport through PMPSi chain is strongly affected by the formation of polarons: the hole is self-trapped in a potential formed by local chain distortion and the charge transport is conditioned by the dynamic change of the polaron potential.

5. Conclusion

The objective of this paper was to investigate the charge carrier transport in PMPSi both experimentally (by using time-resolved THz spectroscopy) and theoretically (employing DFT and other molecular modelling methods). Due to our specific and complex methods we were able to get a deep insight into the charge movement. The transport on the picosecond time scale is due to holes with an on-chain mobility of $0.02 \text{ cm}^2 \text{ V}^{-1} \text{ s}^{-1}$. The mobility is low owing to the hole self-trapping, very probably caused by local chain distortions. The charge mobility value is in agreement with the value obtained by time-resolved microwave photoconductivity and is also supported by the calculations using theoretical chemistry methods. From our theoretical and experimental results we can conclude that charge (delocalised hole) transport through the PMPSi chain is affected by the formation of polarons: the hole is self-trapped in a potential formed by local chain distortion. Charge transport is thus conditioned by

the dynamic change of the polaron potential accompanying the hole motion, which strongly reduces drift mobility.

Acknowledgements

This work was supported by the Grant Agency of the Academy of Sciences of the Czech Republic (Grant No. KAN401770651), by the Academy of Sciences of the Czech Republic (Grant No. AVOZ10100520), by the Czech Science Foundation (Grants No. 202/09/P099, P304/10/1951, 203/08/1594), by the Ministry of Education, Youth and Sports (Grant No. 1041/2006-32 and LC512) and by the European Commission through the Human Potential Programme (Marie-Curie RTN BIMORE, Grant No. MRTN-CT-2006-035859).

References

- 1 N. J. Tao, *Nat. Nanotechnol.*, 2006, **1**, 173.
- 2 F. C. Grozema, L. D. A. Siebbeles, J. M. Warman, S. Seki, S. Tagawa and U. Scherf, *Adv. Mater.*, 2002, **14**, 228.
- 3 S. Nešpůrek, G. Wang and K. Yoshino, *J. Optoelectron. Adv. Mater.*, 2005, **7**, 223.
- 4 R. D. Miller and J. Michl, *Chem. Rev.*, 1989, **89**, 1359.
- 5 S. Nešpůrek, H. Valerian, A. Eckhardt, V. Herden and W. Schnabel, *Polym. Adv. Technol.*, 2001, **12**, 306.
- 6 F. A. Hegmann, O. Ostroverkhova and D. G. Cooke, in *Photophysics of Molecular Materials*, Wiley-VCH Verlag GmbH & Co. KGaA, Weinheim, 2006, pp. 367–428.
- 7 H. Němec, P. Kužel and V. Sundström, *Phys. Rev. B: Condens. Matter Mater. Phys.*, 2009, **79**.
- 8 H. Němec, P. Kužel and V. Sundström, *J. Photochem. Photobiol. A* (in press).
- 9 C. Schmuttenmaer, *Chem. Rev.*, 2004, **104**, 1759.
- 10 E. Hendry, M. Koeberg, J. M. Schins, H. K. Nienhuys, V. Sundström, L. D. A. Siebbeles and M. Bonn, *Phys. Rev. B: Condens. Matter Mater. Phys.*, 2005, **71**.
- 11 P. Prins, F. C. Grozema, J. M. Schins and L. D. A. Siebbeles, *Phys. Status Solidi B*, 2006, **243**, 382.
- 12 J. W. Mintmire, *Phys. Rev. B*, 1989, **39**, 13350.
- 13 S. L. Dexheimer, *Terahertz Spectroscopy—Principles and Applications*, CRC Press, Boca Raton, 2008.
- 14 L. Fekete, P. Kužel, H. Němec, F. Kadlec, A. Dejneka, J. Stuchlík and A. Fejfar, *Phys. Rev. B: Condens. Matter Mater. Phys.*, 2009, **79**, 115306.
- 15 A. Nahata, A. S. Weling and T. F. Heinz, *Appl. Phys. Lett.*, 1996, **69**, 2321.
- 16 S. Nešpůrek and A. Eckhardt, *Polym. Adv. Technol.*, 2001, **12**, 427.
- 17 P. Kužel, F. Kadlec and H. Němec, *J. Chem. Phys.*, 2007, **127**, 024506.
- 18 B. N. Flanders, R. A. Cheville, D. Grischkowsky and N. F. Scherer, *J. Phys. Chem.*, 1996, **100**, 11824.
- 19 Accelrys Software Inc. (2003) Materials Studio Modeling Environment, Release 4.3 documentation. Accelrys Software Inc., San Diego.
- 20 J. R. Maple, M. J. Hwang, T. P. Stockfisch, U. Dinur, M. Waldman, C. S. Ewig and A. T. Hagler, *J. Comput. Chem.*, 1994, **15**, 162.
- 21 H. Tachikawa, *J. Phys. Chem. A*, 2007, **111**, 10134.
- 22 S. Irie and M. Irie, *Macromolecules*, 1997, **30**, 7906.
- 23 M. J. Frisch, *et al.*, *Gaussian 09 (Revision A.02)*, Gaussian, Inc., Pittsburgh, PA, 2009.
- 24 A. D. Becke, *J. Chem. Phys.*, 1993, **98**, 5648.
- 25 Y. Takeshi, P. T. David and C. H. Nicholas, *Chem. Phys. Lett.*, 2004, **393**, 51.
- 26 Y. Tawada, T. Tsuneda, S. Yanagisawa, T. Yanai and K. Hirao, *J. Chem. Phys.*, 2004, **120**, 8425.
- 27 P. C. Hariharan and J. A. Pople, *Theor. Chim. Acta*, 1973, **28**, 213.
- 28 H. F. King, R. E. Stanton, H. Kim, R. E. Wyatt and R. G. Parr, *J. Chem. Phys.*, 1967, **47**, 1936.
- 29 I. Kratochvílová, S. Nešpůrek, J. Šebera, S. Záliš, M. Pavelka, G. Wang and J. Sworakowski, *Eur. Phys. J. E*, 2008, **25**, 299.

- 30 I. Kratochvílová, T. Todorcev, K. Král, H. Němec, M. Bunček, J. Šebera, S. Záliš, Z. Vokčov, V. Sychrovský, L. Bednárová, P. Mojzeš and B. Schneider, *J. Phys. Chem. B*, 2010, **114**, 5196.
- 31 I. Kratochvílová, K. Král, M. Bunček, A. Višková, S. Nešpůrek, A. Kochalska, T. Todorcev, M. Weiter and B. Schneider, *Biophys. Chem.*, 2008, **138**, 3.
- 32 J. Šebera, S. Nešpůrek, I. Kratochvílová, S. Záliš, G. Chaidogiannos and N. Glezos, *Eur. Phys. J. B*, 2009, **72**, 385.
- 33 S. Záliš, I. Kratochvílová, A. Zambova, J. Mbendyo, T. E. Mallouk and T. S. Mayer, *Eur. Phys. J. E*, 2005, **18**, 201.
- 34 V. Coropceanu, J. Cornil, D. A. da Silva Filho, Y. Olivier, R. Silbey and J.-L. Brédas, *Chem. Rev.*, 2007, **107**, 926.
- 35 E. J. Bylaska, et al., *NWChem, A Computational Chemistry Package for Parallel Computers, version 5.1*, Pacific Northwest National Laboratory, Richland, WA, 2007.
- 36 R. A. Marcus and N. Sutin, *Biochimica Biophysica Acta*, 1985, **35**, 437.
- 37 J. R. Bolton, N. Mataga and G. McLendon, in *Electron Transfer in Inorganic, Organic and Biological Systems*, American Chemical Society, Washington, DC, 1991.
- 38 A. Farazdel, M. Dupuis, E. Clementi and A. Aviram, *J. Am. Chem. Soc.*, 1990, **112**, 4206.
- 39 A. Datta, S. Mohakud and S. K. Pati, *J. Mater. Chem.*, 2007, **17**, 1933.
- 40 A. Datta, S. Mohakud and S. K. Pati, *J. Chem. Phys.*, 2007, **126**, 144710.
- 41 R. A. Marcus, *Rev. Mod. Phys.*, 1993, **65**, 599.
- 42 P. F. Barbara, T. J. Meyer and M. A. Ratner, *J. Phys. Chem.*, 1996, **100**, 13148.
- 43 D. A. da Silva Filho, Y. Olivier, V. Coropceanu, J.-L. Brédas and J. Cornil, *Theoretical Aspects of Charge Transport in Organic Semiconductors: A Molecular Perspective*, in *Organic Field-Effect Transistors*, ed. Z. Bao, J. Locklin, CRC, Boca Raton, FL, 2007, ch. 1.
- 44 J. Cornil, J.-L. Brédas, J. Zaumseil and H. Sirringhaus, *Adv. Mater.*, 2007, **19**, 1791.
- 45 A. Troisi, *Adv. Mater.*, 2007, **19**, 2000.
- 46 S.-Z. Weng, P. Shukla, M.-Y. Kuo, Y.-C. Chang, H.-S. Sheu, I. Chao and Y.-T. Tao, *ACS Appl. Mater. Interfaces*, 2009, **1**, 2071.
- 47 L. Viani, Y. Olivier, S. Athanasopoulos, D. A. da Silva Filho, J. Hulliger, J.-L. Brédas, J. Gierschner and J. Cornil, *ChemPhysChem*, 2010, **11**, 1062.
- 48 V. Coropceanu, J. M. André, M. Malagoli and J. L. Bredas, *Theor. Chem. Acc.*, 2003, **110**, 59.
- 49 S. Nešpůrek, V. Cimrová, J. Pfleger and I. Kmínek, *Polym. Adv. Technol.*, 1996, **7**, 459.
- 50 V. Cimrová, I. Kmínek, S. Nešpůrek and W. Schnabel, *Synth. Met.*, 1994, **64**, 271.
- 51 S. Nešpůrek, F. Schauer, A. Kadashchuk and I. I. Fishchuk, *J. Non-Cryst. Solids*, 2007, **353**, 4474.
- 52 L. Onsager, *Phys. Rev.*, 1938, **54**, 554.
- 53 To reduce the time required for the experiments, we measured the THz waveforms in a very short window (3 ps). The Fourier transformation then results in the characteristic artificial “ringing” in the measured spectra which negatively influences the quality of the fits.
- 54 I. Chen, J. Mort and J. H. Tabak, *IEEE Trans. Electron Devices*, 1972, **19**, 413.
- 55 S. Nešpůrek and K. Ulbert, *Cesk. Cas. Fyz.*, 1975, **25A**, 144.
- 56 H. Frey, M. Möller, M. P. de Haas, N. J. P. Zenden, P. G. Schouten, G. P. van der Laan and J. M. Warman, *Macromolecules*, 1993, **26**, 89.
- 57 S. Nešpůrek, V. Herden, M. Kunst and W. Schnabel, *Synth. Met.*, 2000, **109**, 309.
- 58 S. Nešpůrek, J. Sworakowski, A. Kadashchuk and P. Toman, *J. Organomet. Chem.*, 2003, **685**, 269.
- 59 H. Němec, H.-K. Nienhuys, E. Perzon, F. Zhang, O. Inganäs, P. Kužel and V. Sundström, *Phys. Rev. B: Condens. Matter Mater. Phys.*, 2009, **79**, 245326.
- 60 F. C. Grozema and L. D. A. Siebbeles, *Int. Rev. Phys. Chem.*, 2008, **27**, 87.
- 61 S. Nešpůrek, J. Nožár, A. Kadashchuk and I. I. Fishchuk, *J. Phys.: Conf. Ser.*, 2009, **193**, 012108.
- 62 I. Y. Zhang, J. Wu and X. Xu, *Chem. Commun.*, 2010, **46**, 3057.
- 63 J. L. Brédas, J. Ph. Calbert, D. A. da Silva Filho and J. Cornil, *Proc. Natl. Acad. Sci. U. S. A.*, 2002, **99**, 5804.